OCEANOLOGICA ACTA - VOL. 21 - N° 1

Tidal dynamics of the south-west lagoon of New Caledonia: observations and 2D numerical modelling

Tide
Model
Two-dimensional
New Caledonia
Residual current

Marée
Modèle
Bidimensionnel
Nouvelle-Calédonie
Courant résiduel

Pascal DOUILLET

ORSTOM, Centre de Nouméa, BP A5, Nouméa, New Caledonia.

Received 10/09/96, in revised form 07/05/97, accepted 15/05/97.

ABSTRACT

The purpose of this paper is to determine, with the aid of a two-dimensional model, the depth-averaged tidal stream in the south-west lagoon of New Caledonia. A description based on field data is given first. Coastal sea level and open-sea data (bottom pressure, currents) are harmonically and spectrally analysed. The first-order dynamics of this lagoon are dominated by semi-diurnal tides. Except for the passes, diurnal tides and currents are weak, only the two tidal harmonics M_2 and S_2 are subsequently investigated.
A numerical model is used to provide a coherent and dense picture of the tidal dynamics of M_2 and S_2 and their variability. The validity of the model is assessed by comparing its results with measured sea level and current data. Amplitudes and phase-lags of the M_2 tide increase from south to north. M_2 currents are maximum in the south and in the passes. S_2 amplitudes increase from south to north but slower than M_2. S_2 phases spread from north-west to south-east.
Using model results, the long-term movement of the water mass due to tidal influence is estimated by calculating the residual Lagrangian velocity. © Elsevier, Paris.

RÉSUMÉ

Circulation due à la marée dans le lagon sud-ouest de Nouvelle-Calédonie: observations et modélisation bidimensionnelle.

Le but de cet article est de déterminer, à l'aide d'un modèle bidimensionnel, les courants dus à la marée dans le lagon sud-ouest de Nouvelle-Calédonie. Une description à partir des différentes données récoltées est tout d'abord présentée. Des analyses harmoniques et spectrales de la marée et des courants ont été réalisées. Il en résulte que les ondes de marée semi-diurnes sont prépondérantes. En dehors des passes, les courants dus aux ondes diurnes sont faibles, et seules les ondes de M_2 et S_2 sont ensuite étudiées.
Un modèle numérique est utilisé afin de donner une couverture suffisamment dense et cohérente de la dynamique des ondes M_2 et S_2. Sa validité a été assurée en comparant ses résultats aux mesures. Il montre que l'amplitude et la phase de M_2 croissent du sud vers le nord. De même, l'amplitude de S_2 croît du sud vers le nord mais plus lentement que M_2. Par contre, la phase de S_2 se propage du nord-ouest au sud-est.
A partir des résultats du modèle, le mouvement à long terme des masses d'eau sous l'influence de la marée est déterminé en calculant les vitesses résiduelles lagrangiennes. © Elsevier, Paris.

Oceanologica Acta, 1998, **21**, 1, 69-79.

INTRODUCTION

In 1984, ORSTOM (Institut Français de Recherche Scientifique pour le Développement en Coopération) initiated an extensive study of lagoons around New Caledonia, located in the South Pacific, (LAGON experiment). One of its objectives was to determine the fundamental processes affecting the ecosystems.

The lagoons of New Caledonia are extensive, covering a total area of approximately 24 000 km^2 (small chart Fig. 1). These lagoons may be separated geographically. Most of the population is located along the shore of the south-west lagoon where Nouméa, the main city, is located. Geomorphologically, this lagoon is funnel-shaped, with the coast as one side and the barrier reef as the other (Fig. 1). The mean depth of this small inland sea is between 15 and 20 m. From north to south, its length is about 150 km. Its width tapers from 40 km in the south to about 2 km in the north. The barrier reef is cut by deep passes and its crest emerges during the lowest tides.

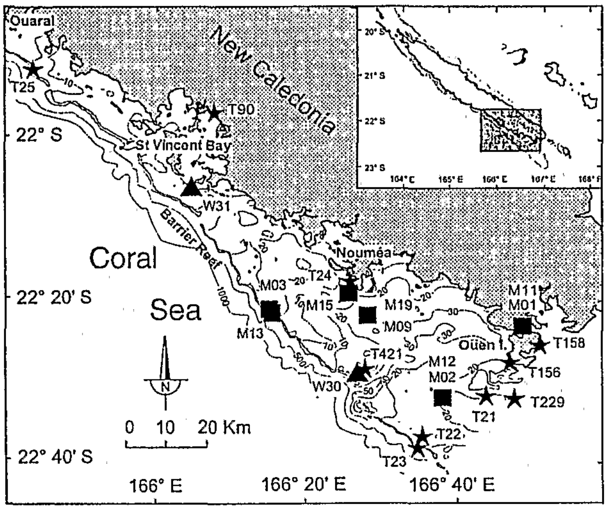

Figure 1

The south-west lagoon of New Caledonia. Location of the sea-level sites (★), currentmeter moorings (■) and weather stations (▲).

Relatively few measurements and studies have been devoted to the dynamics of the south-west lagoon. The first study of current circulation was carried out by ORSTOM and the Flinders University of South Australia in 1975. Over a five-week period, currents and sea-levels were measured around Nouméa. The report (Jarrige *et al.*, 1975) shows the influence of wind and tides on the generation of the circulation. In conclusion the authors proposed three schemes of circulation for three conditions of wind and tide: weak wind and spring tide forcing; strong trade wind forcing; weak wind and neap tide forcing. Morlière (Morlière and Crémoux, 1981; Morlière, 1985) deployed some currentmeters around Nouméa, but the objective was only to obtain measurements for Nouméa's sewerage project. Rougerie (1986) has reported a number of studies, performed on four permanent transects (extending from the coast to the barrier reef) along which temperature and salinity were measured.

The data from these studies are too scant to define a general circulation scheme for the south-west lagoon. Consequently, one of the objectives of the LAGON experiment was to determine its general circulation. From the start, it was decided that the long term goal was to build a numerical model of the currents in the whole of the lagoon. With this in mind, a series of cruises was performed from 1988 to 1990, and completed with data from SHOM (Service Hydrographique et Océanographique de la Marine).

The major objective was to establish the tidal circulation in the south-west lagoon, which had up to that time been misunderstood. The tide, because it is a permanent phenomenon, is one of the most important factors, essential in the analysis of particle transfer and in the interpretation of sedimentology. Moreover, a number of phenomena in biology, *i.e.* the transport of fish eggs and larvae, cannot be analysed without a precise knowledge of the tidal circulation. The objective of this paper is to present these results.

The second part of the paper is concerned with the analysis of coastal sea levels measured by SHOM, and the data (bottom pressure and currents) collected by ORSTOM during various cruises. Harmonic and spectral analyses will be used for these data. Wind effects on the lagoon are also examined.

The third part, the result from a numerical model of M_2 and S_2 tides in the south-west lagoon is presented. Firstly the depth-averaged type of 2D model is briefly described. This numerical model is used to provide a coherent and dense picture of the tidal dynamics. The validity of the model is carefully assessed. A comparison between measured and modelled results is then given, followed by co-tidal charts of the M_2 and S_2 tides and tidal streams. Finally, the residual Lagrangian velocities are presented and interpreted.

MEASUREMENTS

The data

Several databases were used. The main database is a series of measurements done during the LAGON experiment. The measuring instruments were strategically placed in order to develop numerical models of the circulation. From 1988 to 1990, four water-level recorders, three moorings with two currentmeters each (one near the surface, the other at the bottom) and two weather stations were deployed at different points of the lagoon (Fig. 1). These instruments measured at 10-minute intervals sea level, tidal flows, water and air temperature as well as wind velocity. SHOM provided further data which have been used either for the model or for comparison with the results of the model. The final batch of data, on currents, was obtained from the works of Morlière and Crémoux in 1981 and Morlière in 1985.

The locations of the sea level stations used in the following analysis are listed in Table 1*a* and illustrated in Figure 1.

Table 1*a*

Description of bottom pressure data and sea-level gauges.

Location code	Device type	Latitude (°N)	Longitude (°E)	Depth (m)	Instrument depth (m)	Start date	Stop date	No. of usable days	Sampling Interval (s)
M01	Aanderaa RCM7	-22° 23' 06"	166° 48' 08"	36	34	16 Feb. 1989	31 Oct. 1990	606	600
M11	Suber SLS11	-22° 23' 06"	166° 48' 08"	36	4	16 Feb. 1989	31 Oct. 1990	341	600
M02	Aanderaa RCM7	-22° 32' 08"	166° 37' 57"	23	21	23 Nov. 1988	05 Oct. 1990	576	600
M12	Suber SLS11	-22° 32' 08"	166° 37' 57"	23	4	18 Oct. 1988	05 Oct. 1990	440	600
M03	Aanderaa RCM7	-22° 21' 15"	166° 15' 05"	30	28	18 Jan. 1989	31 Oct. 1990	642	600
M13	Suber SLS11	-22° 21' 45"	166 15' 27"	18	4	18 Jul. 1989	31 Oct. 1990	376	600
M15	Aanderaa RCM4	-22° 19' 15"	166° 25' 30"	21	3	24 Nov. 1984	19 Apr. 1985	139	1800
M09	Aanderaa RCM4	-22° 22' 00"	166° 28' 00"	26	20	30 Jan. 1981	04 Mar. 1982	284	1800
M19	Aanderaa RCM4	-22° 22' 00"	166° 28' 00"	26	6	30 Jan. 1981	04 Mar. 1982	312	1800

Table 1*b*

Description of currentmeter data.

Location code	Device type	Latitude (°N)	Longitude (°E)	Depth (m)	Start date	Stop date	No. of usable days	Sampling interval (s)
T21	Aanderaa WRL7	-22° 31' 57"	166° 43' 34"	10	27 Dec. 1988	05 Oct. 1990	645	600
T22	Aanderaa WRL7	-22° 37' 00"	166° 35' 53"	9	12 Oct. 1988	05 Oct. 1990	638	600
T23	Aanderaa WRL7	-22° 38' 24"	166° 34' 48"	15	27 Dec. 1988	12 Sep. 1990	664	600
T25	Aanderaa WRL7	-21° 52' 18"	165° 43' 01"	12	13 Dec. 1988	08 Oct. 1990	664	600
T24 (Nouméa)	sea level gauges	-22° 17' 30"	166° 26' 00"	—				3600
T90 (Tomo)	Sea level gauges	-21° 57' 00"	166° 07' 40"	—	12 Sep. 1966	02 Nov. 1966	44	3600
T156 (Ile Ouen)	Sea level gauges	-22° 27' 42"	166° 46' 36"	—	06 Aug. 1970	05 Oct. 1970	32	3600
T158 (Ouara)	Sea level gauges	-22° 25' 30"	166° 50' 20"	—	22 Jul. 1970	12 May 1975	247	3600
T229 (Mato)	Sea level gauges	-22° 32' 12"	166° 47' 12"	—	20 Mar. 1977	17 Dec. 1977	157	3600
T278 (N'Da)	Sea level gauges	-22° 50' 05"	166° 52' 30"	—	03 Jun. 1977	13 Mar. 1978	110	3600
T421 (Ph. Amédée)	Sea level gauges	-22° 28' 42"	166° 27' 42"	—	18 Feb. 1975	16 Dec. 1975	74	3600

Points T21, T22, T23 and T25 result from the LAGON programme. They were chosen in order to determine the boundary conditions at the south and outside the lagoon for a numerical model. These data needed to be as accurate as possible, and were measured over a two-year span. In order to establish all measurements at precisely the same depth, the water-level recorders were placed in fixed PVC structures. Measurements of sea level, on the outer reef of the south-west lagoon, were made. These first-time measurements were necessary because the existing global ocean co-tidal charts (Schwiderski, 1981) were not sufficiently accurate (one datum per degree square) for our purpose. Nevertheless, these global co-tidal charts were used to define and interpret the tide around New Caledonia. For all the water-level data collected during the LAGON programme, bottom pressure was measured, and corrected

Table 1*c*

Description of the wind data.

Location code	Device type	Latitude (°N)	Longitude (°E)	Start date	Stop date	No. of usable days	Sampling interval (s)
W30	Aanderaa 3100	-22° 29' 03"	166° 26' 45"	06 Mar. 1989	18 Oct. 1990	591	600
W31	Aanderaa 3100	-22° 06' 08"	166° 04' 40"	20 Jul. 1989	07 Nov. 1990	325	600

for atmospheric effect and density to obtain estimates of sea level. The other sea levels, obtained from SHOM, were measured directly rather than estimated from records of bottom pressure. For these, only the harmonic constants are available.

Measurements of tidal flows were made during several ORSTOM cruises (1975, 1981, 1985, 1988–1990). Table 1*b* summarizes the information from each mooring and Figure 1 shows their location. For convenience, the currentmeters located above the bottom have a name beginning with M0 and those located near the suface have a name beginning with M1. More details concerning these measurements can be found in Jarrige *et al.* (1975), Morlière and Crémoux (1981), Morlière (1985), and Douillet *et al.* (1989, 1990).

Wind measurements were collected during ORSTOM cruises in 1988–1990. Table 1*c* and Figure 1 summarize the information from each weather station. A monthly summary was extracted from the ORSTOM cruises of 1988-1990. Two research reports were produced for the 1988-1990 data (Douillet *et al.*, 1989, 1990).

Analysis

The results presented in this part are not intended to be an exhaustive analysis of the measurements, but concentrate on the material required to initialize and validate the model.

Measurements of tides and tidal streams were analysed harmonically using methods developed at SHOM (Simon, 1974; Bessero, 1979). Tidal flows were also analysed spectrally using a method developed by Gonella (1972).

The results of the harmonic analysis for the semi-diurnal and diurnal species are given in Table 2*a* for sea-level and Table 2*b* for currents.

Harmonic analysis of vertical tide

From the harmonic analysis, M_2 is the dominant signal in the tidal waveband (roughly $3 \times K_1$, $5 \times O_1$, $9 \times P_1$, $5 \times N_2$, $3 \times S_2$). The criterion of amplitude ratio $(O_1 + K_1)/(M_2 + S_2)$ shows that the tide is mixed, mainly semi-diurnal. The values measured at points T158, T229, T21, T22 and T421 show that the amplitude of the M_2 constituent increases from the southeastern part of the lagoon towards the interior. The same feature is apparent for the S_2 amplitude, but not for the K_1 amplitude which is the same over most of the lagoon. The co-tidal charts, calculated by Schwiderski (1981), show that the amplitude and phase-lags of the M_2 and S_2 constituents have very different values between the eastern and western coast of New Caledonia, but the variations are very weak for the K_1 constituent, about one centimetre for the amplitude and two degrees for the phase. No significant amplitude was found for quarter-diurnal or higher constituents. They are always lower than 0.5 cm. The phase of M_2 increases from the south-east part to the interior of the lagoon (Table 2*a*, points T158, T229, T21, T22 and T421), but the phase of S_2 decreases. These observations imply a different propagation for the two constituents. Analyses of the two water-level recorders T23 and T25 give an explanation of this difference. The propagation of the M_2 constituent, outside the lagoon, is from south to north whereas the propagation of the S_2 constituent is from north to south. Schwiderski (1981) shows the same results for the propagation of these constituents in the entire New Caledonian area.

Harmonic analysis of tidal flows

Tidal streams are mainly generated by the M_2 constituent. Two other constituents, S_2 and K_1, also contribute to the tidal stream. For the S_2 constituent, the currents are one-third of M_2; and for the K_1 constituent, the currents are generally one-tenth of M_2 ($\approx$ 0.01 m s^{-1}), except for the points M03 and M13. These points are located in a pass. The tidal stream is modified there by the propagation of the K_1 constituent, outside the lagoon, which is probably perpendicular to the barrier reef. The results of Schwiderski (1981) are consistent with these findings. The currents are about 0.07 m s^{-1}, which is larger than in the other parts of the lagoon, but lower than the M_2 constituent (around 0.3 m s^{-1}), and also lower than the S_2 constituent (around 0.1 m s^{-1}). At M01, M11, M03, M13 and M15 stations, some currents are due to quarter-diurnal or higher constituents, but they are at least ten times weaker than M_2. At M03 and M13 stations, the K_1 constituent reaches a higher value than elsewhere. The quarter-diurnal or higher constituents generate at these stations a current which is two or three time weaker than K_1. In the central part (currentmeters M02, M12), the major axis of the ellipse is aligned approximately in the direction of the channel, and the values of the semi-major axes between the surface and the bottom currentmeter are not significantly different. The currentmeters M01 and M11 were not located in the central part of the channel of Ouen Island (for navigational reasons) and current transects perpendicular to the channel show that the current is

Table 2*a*

Diurnal and semi-diurnal constants for bottom pressure and coastal sea level.

Location/ instrument	Analysis period (Days)	O_1 H(m)	O_1 g(°g)	K_1 H(m)	K_1 g(°g)	M_2 H(m)	M_2 g(°g)	S_2 H(m)	S_2 g(°g)	$\frac{O_1+K_1}{M_2+S_2}$
T21	643	0.066	149.1	0.136	191.9	0.354	222.1	0.118	277.1	0.428
T22	636	0.066	149.3	0.136	191.8	0.382	223.2	0.126	272.9	0.398
T23	663	0.064	148.5	0.133	190.2	0.386	227.0	0.136	272.0	0.377
T25	662	0.068	152.8	0.138	191.1	0.377	228.9	0.138	267.5	0.400
T24	730	0.069	148.5	0.138	190.4	0.409	228.1	0.141	274.8	0.376
T90	44	0.067	160.9	0.150	184.0	0.423	234.1	0.135	280.3	0.389
T156	32	0.068	145.5	0.136	191.5	0.376	226.8	0.125	284.5	0.407
T158	247	0.070	147.3	0.138	192.8	0.308	211.3	0.082	282.2	0.533
T229	157	0.061	149.8	0.126	190.3	0.337	218.1	0.103	280.0	0.425
T421	74	0.067	143.7	0.135	191.5	0.397	228.0	0.138	275.4	0.378

Table 2*b*

Diurnal and semi-diurnal constants for currents.

Location/ instrument	Instrument depth/ water depth (m)	Analysis period (Days)	O_1 Semi-major axis (a) (m s^{-1})	O_1 Semi-minor axis (b) (m s^{-1})	O_1 Orientation °North	K_1 Semi-major axis (a) (m s^{-1})	K_1 Semi-minor axis (b) (m s^{-1})	K_1 Orientation °North	M_2 Semi-major axis (a) (m s^{-1})	M_2 Semi-minor axis (b) (m s^{-1})	M_2 Orientation °North	S_2 Semi-major axis (a) (m s^{-1})	S_2 Semi-minor axis (b) (m s^{-1})	S_2 Orientation °North
M01	32/34	599	0.003	0.000	29.4	0.005	-0.001	9.3	0.178	-0.035	25.8	0.069	-0.009	18.9
M11	3/34	621	0.003	0.000	11.2	0.002	-0.001	116.1	0.158	-0.047	35.7	0.059	-0.024	22.5
M02	19/21	559	0.004	0.000	156.0	0.009	0.002	131.2	0.098	-0.011	112.9	0.036	-0.011	116.9
M12	3/21	448	0.005	0.001	131.9	0.012	0.009	118.5	0.109	-0.005	111.1	0.040	-0.012	113.0
M03	30/32	636	0.045	-0.001	43.7	0.070	0.002	38.3	0.280	0.010	38.0	0.099	0.002	36.8
M13	3/18	362	0.045	0.004	79.4	0.073	0.004	86.0	0.316	0.014	88.2	0.103	0.015	87.4
M15	3/20	124	0.006	0.002	148.8	0.007	0.006	164.7	0.139	0.003	150.6	0.034	-0.002	151.6
M09	20/26	234	0.002	-0.001	77.7	0.007	-0.001	132.6	0.040	0.000	110.8	0.015	-0.003	111.0
M19	6/26	262	0.003	0.002	56.8	0.009	0.002	144.2	0.038	0.002	115.5	0.014	-0.004	120.5

stronger in the central part, and that the channel constrains the streams. The tidal streams are weak near Nouméa (M09 and M19), while currentmeter M15, situated in a submarine valley, shows stronger streams owing to the topography. Values of the semi-major axis of 0.01 m s^{-1} have been found for the M_4 constituent, but they are not significant. There is no significant difference between the tidal currents measured near the bottom and those measured near the surface. Most of the time, the bottom current is smaller or equal to the surface current, except for the mooring M01/M11. The currentmeter near the bottom of this latter mooring was located in a slightly more central part of the channel of Ouen Island. The orientations of the semi- major axes for the mooring M03/M13 are different but the two currentmeters were located in a different manner within the pass. These results prove that the tidal stream is barotropic.

Spectral analysis of tidal flows

The spectral analysis was developed following Gonella (1972). For the statistical analysis of the current-meter data, records were set to a maximum of 28 days, long records being divided into several fractions in order to have more degrees of freedom. Figure 2 shows the mean kinetic energy or total spectrum (solid line), the clockwise spectrum (dashed line), and the anticlockwise spectrum (dot-dashed line) of the different current meters.

Like the harmonic analysis, the spectral analysis shows a significant peak for the semi-diurnal frequency of all currentmeters. For the diurnal frequency, some currentmeters show a peak, as for example currentmeter M12, but the mean kinetic is one-fiftieth to one-hundredth of the semi-diurnal frequency. Only M03 and M13 have a significant peak, but it is much weaker than the semi-diurnal peak (one tenth). For the currentmeters M01, M11, M03, M13, and M15, quarter-diurnal or higher frequencies show peaks, but these values are much lower than the semi-diurnal peak. These peaks are of the same order of magnitude as those of the diurnal period. The harmonic analysis shows, however, that the currents generated by the quarter-diurnal or higher constituents are much weaker in Dumbea Pass (M03, M13) than those due to K_1. The clockwise and anticlockwise spectra have the same size for all the currentmeters. The difference between the clockwise and anticlockwise spectra is proportional to the average of the area of the elliptical surface (Gonella, 1972). The currents are therefore almost unidirectional. The mean kinetic energy of the surface currentmeters and of the bottom currentmeters is the same size. As previously shown with the harmonic analysis, the tidal current is barotropic. In conclusion, the results of this analysis are consistent with the results of the previous one, but in this case, M_2 and S_2 cannot be separated.

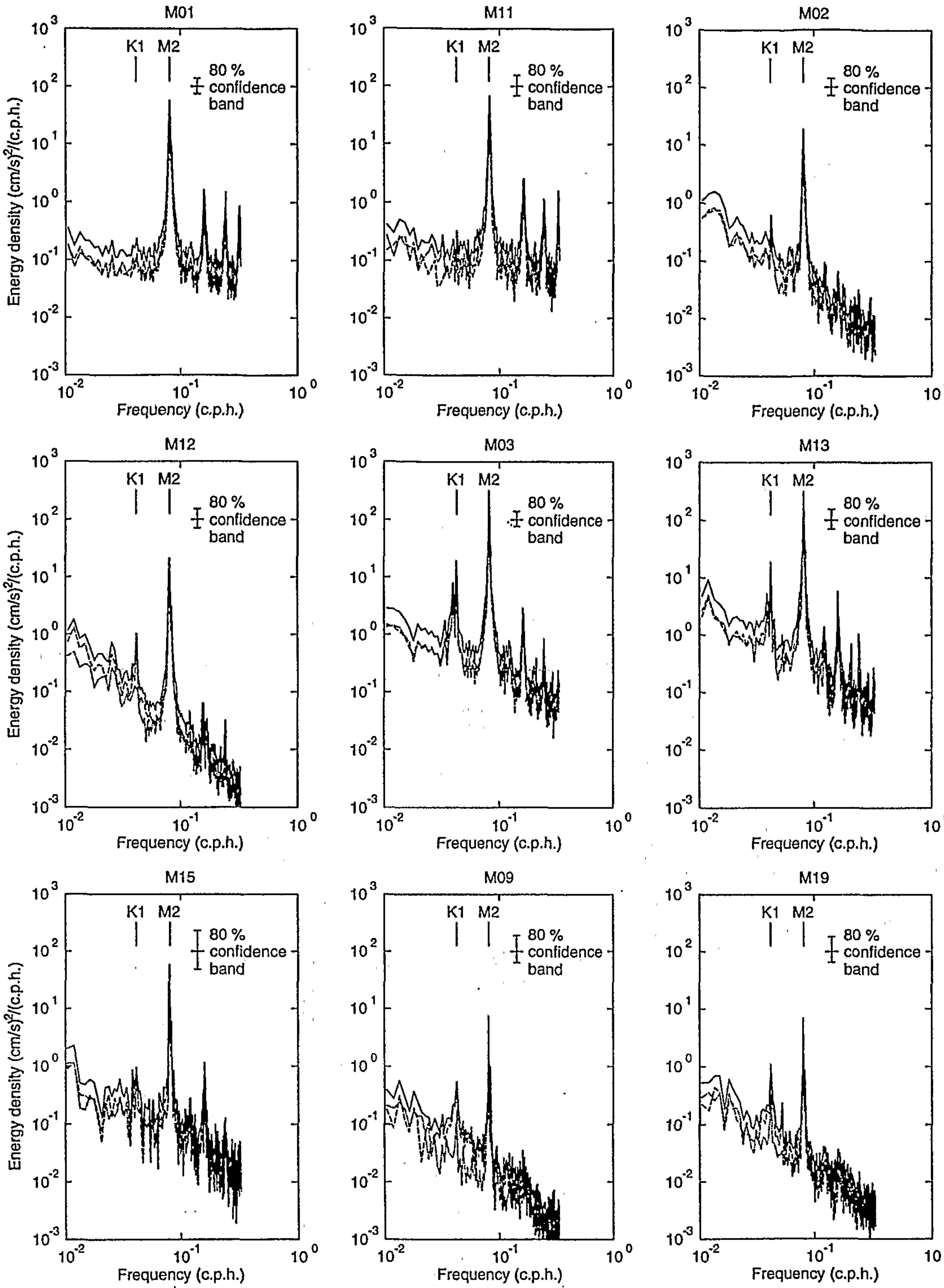

Figure 2

Spectrum of the different currentmeters, total (solid line), clockwise (dashed line) and anticlockwise (dot-dashed line).

Presentation of wind

During more than half of the year (November–May), trade winds blow at around 10 m s^{-1} for W30 and W31. During the austral winter (June–October), winds decrease and the number of days with winds lower than 2 m s^{-1} is significant. In the latter case, wind-generated flows become negligible compared to tidal flows (Douillet *et al.*, 1989, 1990). These results are consistent with those of Jarrige *et al.* (1975). Therefore, two circulation schemes, tides forcing and strong wind forcing, prevail. In this first approach, only weak wind conditions are studied and the numerical model is tidally forced.

NUMERICAL MODELLING OF THE M_2 AND S_2 TIDES

The numerical model

The data analysis of the previous section allows a better knowledge of the tidal circulation in the south-west lagoon of New Caledonia. It is, however, insufficient to determine particle transfers, or to interpret sedimentology, or biological processes. In order to obtain more comprehensive information on the area, barotropic tides were computed using a numerical model. The model is based on Saint-Venant equations, which are obtained by the vertical integration of the Navier-Stokes equations in the case of a homogenous ocean with the very classical Boussinesq and hydrostatic pressure hypotheses. Therefore the set of equations governing the water movement is:

$$\frac{\partial U}{\partial t} + U\frac{\partial U}{\partial x} + V\frac{\partial U}{\partial y} - fV = -g\frac{\partial \zeta}{\partial x} + N_h\left(\frac{\partial^2 U}{\partial x^2} + \frac{\partial^2 U}{\partial y^2}\right) - \frac{\tau_{bx}}{\rho_0\,(h+\zeta)} \qquad (1)$$

$$\frac{\partial V}{\partial t} + U\frac{\partial V}{\partial x} + V\frac{\partial V}{\partial y} + fU = -g\frac{\partial \zeta}{\partial y} + N_h\left(\frac{\partial^2 V}{\partial x^2} + \frac{\partial^2 V}{\partial y^2}\right) - \frac{\tau_{by}}{\rho_0\,(h+\zeta)} \qquad (2)$$

The integration of the equation of continuity yields:

$$\frac{\partial \zeta}{\partial t} + \frac{\partial((h+\zeta)\,U)}{\partial x} + \frac{\partial((h+\zeta)\,V)}{\partial y} = 0 \qquad (3)$$

where $\zeta\,(x,\,y,\,t)$ is the instantaneous sea surface elevation above the undisturbed level, h is the water depth at rest, $U\,(x,\,y,\,t)$, $V\,(x,\,y,\,t)$ are the zonal and meridional depth-averaged velocities, f is the Coriolis parameter, ρ_0 is the density of sea water, g is the acceleration due to gravity, τ_{bx}, τ_{by} are the components of quadratic bottom friction:

$$\tau_{bx} = g\,\frac{\sqrt{U^2+V^2}}{K_r^2\,(h+\zeta)^{1/3}}\,U \qquad \tau_{by} = g\,\frac{\sqrt{U^2+V^2}}{K_r^2\,(h+\zeta)^{1/3}}\,V$$

and K_r is the Strikler coefficient equal to 30 $m^{-1/3}\,s^{-1}$, N_h is the turbulent horizontal diffusion equal to 85 $m^2\,s^{-1}$.

The numerical model is a finite-difference scheme using an ADI (Alternating Direction-Implicit) method. The code used was developed by Salomon (Lazure and Salomon, 1991) and includes automatic treatment of wetting and drying. The critical time step estimated by extracting only the acceleration and bottom friction terms from the equations, is given by:

$$\Delta t < \frac{2\,g\,(\Delta x)^2}{K_r^2\,(h+\zeta)_{\max}|U_{\max}|}$$

where $|U_{\max}|$ is the maximum rate of the tidal stream.

Discretization in equations 1 to 3 is carried out on an Arakawa C grid, slightly modified in so far as the depths are indicated at the same location as the velocity components (Fig. 3).

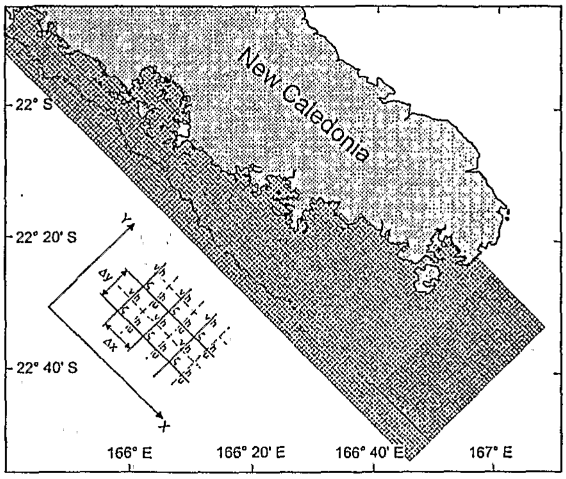

Figure 3

Domain of numerical simulation. The grid scheme is presented. The grey area is an extended area of 50 m depth.

The coastal boundary conditions are simply written by imposing a zero flux across the coastline. For the open boundaries, elevations and a condition of radiation on velocities are specified at each grid point.

Geographically, the domain of simulation is bounded to the west by an open boundary which is a straight line of depth greater than 1000 m (Fig. 1). The extension in the southern part has never been surveyed, and a uniform depth of 50 m has been assumed (Fig. 3, grey area). The grid of computation has a uniform spacing of 1000 m. This spacing has been chosen as a compromise between the available computer power and the resolution necessary to represent geomorphologic features (pass, coast, canyon). The number of grid-points is 171 × 55. The estimate of the stability criterion is in agreement with the range of the time-step limit found during different numerical experiments. In deeper regions inside the lagoon (H = 40 m), the strength of the current remains relatively strong (about 0.5 m s^{-1}), therefore the time step is 150 s.

RESULTS

Comparison between modelled and measured data

Computed amplitudes and phase-lags of the M_2 and S_2 tides (Table 3) may be compared with measured amplitudes and phase-lags (Table 2*a*). The amplitudes and phase-lags of the various constituents are computed by the model over two tidal cycles next to a nine-day simulation period. Sea level data are used only to determine the boundary

Table 3

Modelled amplitudes and phase-lags of M_2 and S_2 tides.

	M_2			S_2		
Location Model	Semi-major axis (a) (m s^{-1})	Semi-minor axis (b) (m s^{-1})	Orientation °North	Semi-major axis (a) (m s^{-1})	Semi-minor axis (b) (m s^{-1})	Orientation °North
M01/M11	0.220	0.013	58.7	0.069	-0.003	59.2
M02/M12	0.140	0.004	115.3	0.049	-0.012	118.7
M03/M13	0.239	0.006	45.2	0.097	-0.004	42.2
M15	0.128	-0.005	141.9	0.038	0.001	139.4
M09/M19	0.049	0.004	115.1	0.016	-0.008	109.0

conditions, but are in no way used to constrain the model within the study zone.

The main features of the sea level are reproduced quite well.

The trend of the M_2 amplitude, minimum at T158 and maximum at T90 with an increase between these two points, is confirmed. The computed sea level is slightly overestimated (by + 0.006 m) for the point T158. This difference may come from an insufficient determination of the southern boundary condition. The agreement is much better for the other points.

The M_2 computed phases agree quite well with the measured data. The measured and computed values at T158 show a difference of 2.7 degrees but this point is near the south-west boundary where the tide is not perfectly known. T421 and T24 have a difference of 0.9 degrees. T421 was measured for only 74 days but with an interruption of several months inducing an approximated phase. Point T24 is located in the harbour of Nouméa near a small channel and therefore cannot be included in the model.

In the same way, the correspondence of S_2 amplitudes between measurement and model is excellent except for the T90 point which has only 44 days of measurement, a number considered insufficient for a good analysis.

The agreement for the S_2 phases is satisfactory in the southern part. The discrepancies between points T421 and T90 are probably linked to the limited span of measurement at these points and to the influence of the pass for the T421 point.

Computed currents (Table 4) may be compared with measured currents (Table 2*b*) for the five sites, but the model gives only a mean current from the surface to the bottom.

The agreement of the amplitude of the current is nevertheless quite good for M_2 and S_2. The computed current is slightly overestimated at points M02/M12 and M01/M11, and underestimated at point M03/M13. For the phase, the agreement is excellent except for points M01/M11 and M03/M13. These differences may be attributed to various origins. First, the bathymetry of the lagoon has great spatial variations and cannot be perfectly represented by a spacing grid of 1000 m. For instance, points M03 and M13, separated by 500 m, are located in the same grid cell. Consequently, large local variations of current rate cannot be perfectly calculated by a model at this scale. This illustrates the difference between measurements, which are local, and modelled data, which represent an average over a cell. Second, a finite-difference model locally distorts the bathymetry in the vicinity of the canyon, thus explaining the error in orientation of the ellipses at points M01/M11 and M03/M13.

Table 4

Semi-diurnal constants for currents computed by the model.

	M_2		S_2	
Location/ model	H(m)	g(°g)	H(m)	g(°g)
T21	0.356	221.7	0.117	277.7
T22	0.381	223.7	0.126	273.9
T23	0.386	227.0	0.136	272.0
T25	0.377	228.9	0.138	267.7
T24	0.403	228.9	0.143	274.2
T90	0.427	234.4	0.155	273.9
T156	0.371	227.1	0.129	279.6
T158	0.314	214.0	0.083	282.6
T229	0.341	218.1	0.106	278.8
T421	0.391	227.1	0.136	273.3

Co-tidal charts

The results of the numerical model are presented as co-tidal charts on Figures 4 and 5.

M_2 constituent. The M_2 sea level patterns have already been described above. The amplitude (Fig. 4*a*) increases regularly from south to north up to St. Vincent Bay. In the northern lagoon, the influence of the external tide is obvious. In all passes, except the most southern one, the results show a penetration of the M_2 tide into the lagoon. Like the amplitude, the phase (Fig. 4*b*) increases from south to north. Both charts show that the M_2 constituent comes into the lagoon from the south, and that phase and amplitude vary rapidly across the reef located west of Ouen Island. North of St. Vincent Bay, the tide comes from the exterior and it seems to be independent from the south part. The amplitude increases from north to south.

The M_2 currents (Fig. 4*c*) are never very strong inside the lagoon (0.2 m s^{-1} maximum). In the southern part of the lagoon, the streams tend to align along the lagoon axis. The amplitude of this current tends to decrease from the south to the north and the current is weaker north of Ouen Island which is deeper than other parts of the lagoon. On the west side of this island, the direction of the major axis of the currents turns, owing to the presence of a reef near Ouen Island. In the passes the current is generally strong and almost rectilinear. The ellipses tend to become circular inside the lagoon, near the passes. This phenomenon may be linked either to the presence of very deep river-beds which extend from the coast to the passes or the combination of the though-pass oriented ellipses with the along-lagoon oriented ellipses. In front of Nouméa, the

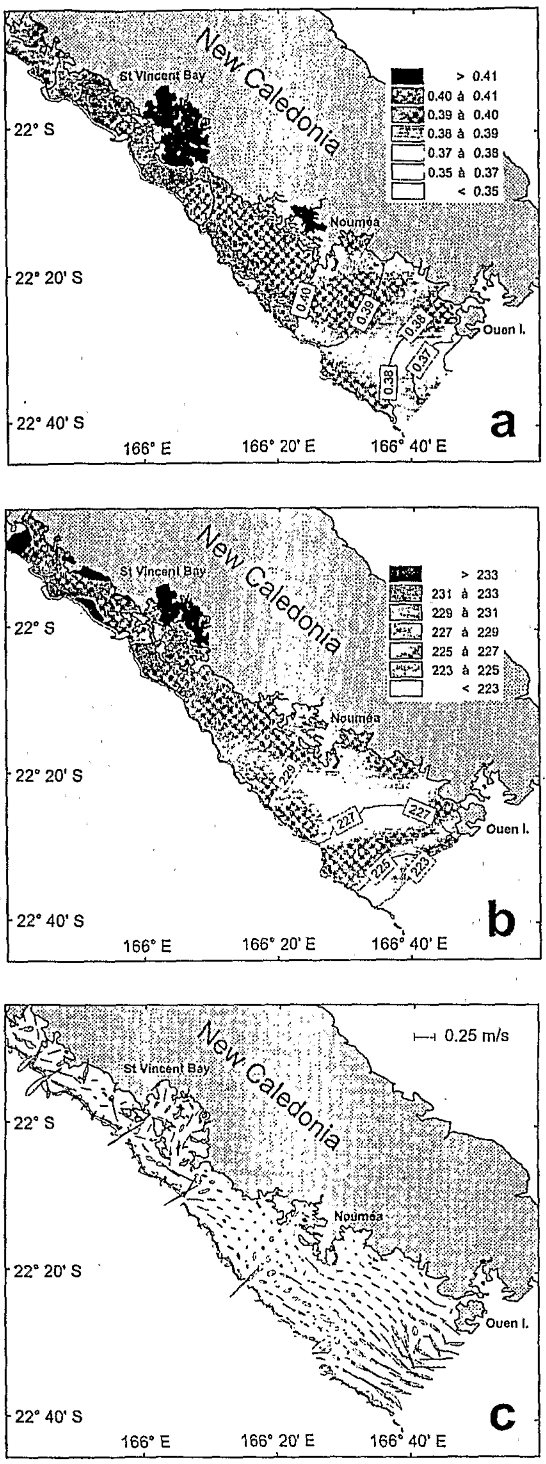

Figure 4

Model simulation of the M_2 constituent. (a) amplitudes, (b) phase-lags, (c) ellipses of the currents.

acceleration of the current is obvious as shown by data from mooring M09/M19. At this point there is a channel between the coast and a reef which is shallower than in the north and in the south (Fig. 1).

S_2 constituent. Figures 5*a* and 5*b* give a picture of the S_2 levels inside the lagoon. As for M_2, the amplitude increases regularly from south to north, and varies rapidly around the reef located west of Ouen Island. North of Nouméa, the increase becomes negligible, 0.01 m between Nouméa and St. Vincent Bay, and practically non-existent north of that bay. The propagation inside the lagoon is from north-west to south-east, the opposite of the M_2 constituent. As shown previously, and as the results of Schwiderski (1981) indicate, outside the lagoon, the S_2 tide propagates from north to south while the tide M_2 propagates from south to north. Other results from SHOM show that the S_2 tide also penetrates the lagoon from the south but not with exactly the same direction as M_2.

As previously mentioned in the data analysis, the S_2 currents (Fig. 5*c*) are weak over most of the lagoon (order 0.03 m s^{-1}), but they may be strong locally in the passes where they can reach 0.1 m s^{-1}. In the southern part of the lagoon, the ellipses are more circular than for M_2. In the passes, the streams are more rectilinear. As for the M_2 current, west of Ouen Island, the direction of the major axis of the currents turns, owing to the presence of a reef near this island.

Lagrangian residual velocity

Long-term transportation of dissolved matter is generally poorly described by the Eulerian mean velocity (*i.e.* at a fixed position) because the latter can differ greatly from the Lagrangian mean velocity (*i.e.* following a marked particle). The difference was termed Stokes velocity by Longuet-Higgins (1969). Using a numerical model, it is straightforward to evaluate the tracks of particles by numerical integration and bilinear interpolation and thus determine the Lagrangian mean velocity. A known drawback of this kind of computation is that the Lagrangian residual mean velocity for one starting position varies with the starting time (Foreman *et al.*, 1992).

This difficulty may be avoided. During a semi-diurnal tidal cycle, the trajectory of a water parcel is a curve and it is possible to calculate the mean position (*i.e.* the barycentre) of the track. For one particle, the movement of the barycentre represents the Lagrangian mean motion. In a more mathematical formalism, it is possible to consider the instantaneous position $\vec{x}(t)$ of a water column as the sum of a mean position $\vec{X}(t)$ (*i.e.* tidally averaged) and a perturbation $\vec{\xi}(t)$ which describes oscillating tidal movement. That is:

$$\vec{x}(t) = \vec{X}(t) + \vec{\xi}(t)$$

where

$$\vec{X}(t) = \frac{1}{T} \int_{t-T/2}^{t+T/2} \vec{x}(x,\, t)\, dt$$

and

$$\int_{t-T/2}^{t+T/2} \vec{\xi}(x,\, t)\, dt = 0$$

The long-term movement is defined by the progressive displacement of the mean position from one cycle to the next. An approximation of this concept (*i.e.* the barycentric method as described in Salomon *et al.*, 1988 and Garreau, 1993) is performed herein. The reader will find some theoretical considerations in the work of Andrew and McIntyre (1978). The result is a velocity field independent of starting time.

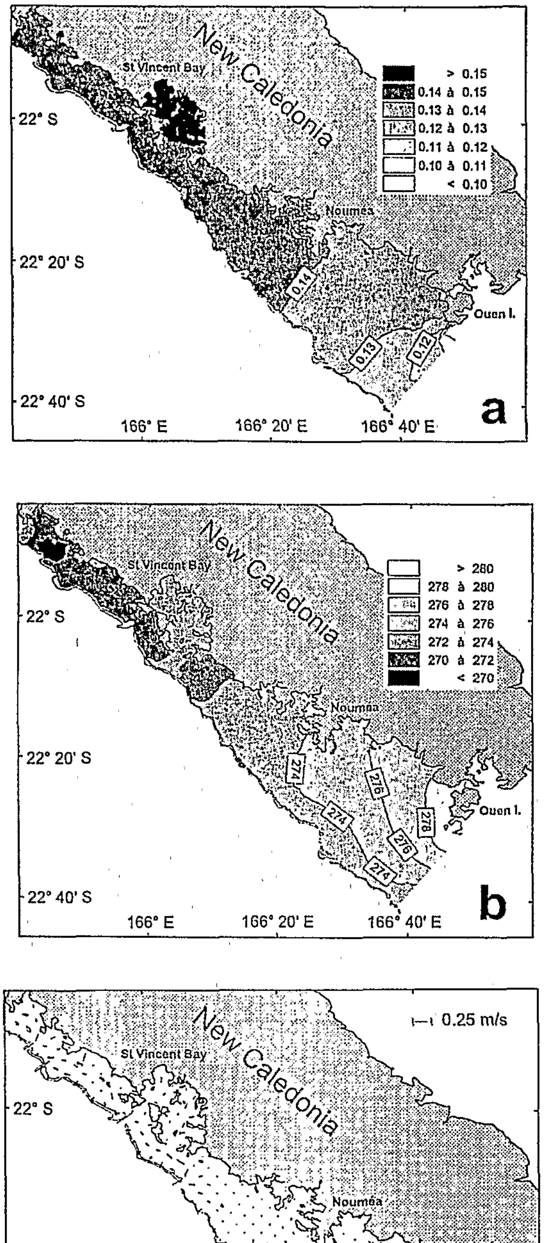

Figure 5

Model simulation of the S_2 constituent. (a) amplitudes, (b) phase-lags, (c) ellipses of the currents.

M_2 constituent. The Lagrangian residual velocity (Fig. 6) can locally reach 0.03 m s^{-1}, but is generally close to 0.01 m s^{-1}. The water mass enters the lagoon in the south between Ouen Island and the barrier reef where the Lagrangian residual current is strongest. This mass is divided into two parts: one flows out of the lagoon through the pass, the other remains in the lagoon and flows northwards and eastwards, and finally leaves the lagoon by the pass in front of Nouméa. The water mass from the south is totally separated from the northern one and cannot enter that part of the lagoon. There is a vortex on the west side of Ouen Island that is generated by a shallow reef (Fig. 6, zoom *c*). It is a classical cape effect. Near the coast and in an area north of Ouen Island, the residual currents are weak. The residence time of the water masses in these areas is longer than in the other parts of the lagoon. On both sides of the passes, vortices are clearly visible. This is due to topographic variations, the vortices being located precisely over deep fossil river-beds which extend from the coast to the passes. The zoom *a* shows that, in the pass, the Lagrangian residual velocity is directed towards the interior, whereas the zoom *b* shows that the Lagrangian residual velocity heads towards the exterior of the lagoon. The former residual is in a zone where the tide comes from the exterior. The latter residual is found in a zone where the water mass comes from the south. It cannot go northwards, being blocked by the water masses descending southwards, and the only escape route is through the passes. The convergence area between the north and the south of

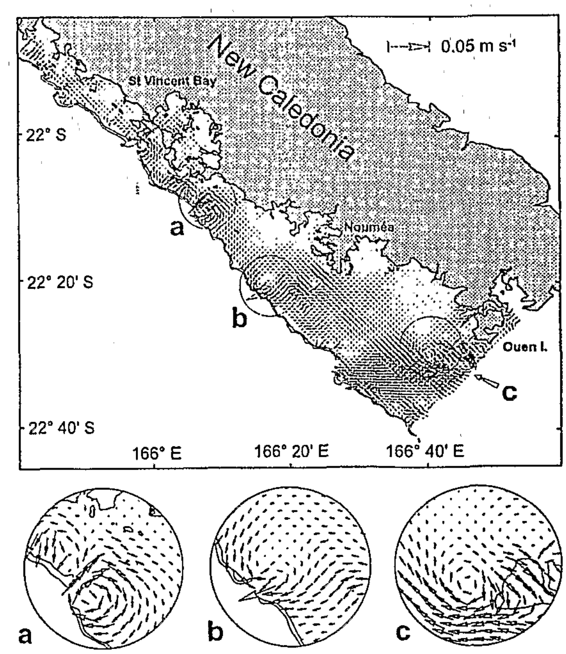

Figure 6

Lagrangian residual velocity fields of the M_2 constituent.

the lagoon is located between these two passes. South of St. Vincent Bay, areas with weak Lagrangian residual current coincide with zones of muddy sediment. Nearshore, in the zones of increasing Lagrangian residual current, the mud content of the sediment decreases (Chardy *et al.*, 1988; Debenay, 1987).

S_2 constituent. The Lagrangian residual velocity of S_2 is ten times smaller than the M_2 Lagrangian residual velocity and is not shown here.

CONCLUSIONS

The tidal characteristics of the south-west lagoon of New Caledonia have been investigated for the diurnal and semi-diurnal species. The semi-diurnals are the most energetic. The influence of the diurnal tides is weak.

The investigation includes the analysis of measurements (coastal sea level, bottom pressure and current) and the numerical modelling of M_2 and S_2.

In the semi-diurnal species, amplitudes are amplified from south to north, but more weakly for S_2 than for M_2. The phase of M_2 increases northward and the phase of S_2 increases from north-west to south-east. The M_2 currents are the greatest (of the order 0.2 m s^{-1}) in the southern part of the lagoon and in the passes. Tidal ellipses are generally aligned in the direction of the channels except in the passes; they are essentially rectilinear, except over the fossil river beds. The S_2 currents are weak over most of the lagoon (of the order 0.03 m s^{-1}).

The numerical model described herein is an efficient tool for obtaining an overview of the instantaneous currents but also, using Lagrangian residual velocity, the only means of determining the long-term transport of particles under tidal influence.

The next task is to include wind forcing. To take into account the vertical structure of currents, a three-dimensional model is necessary and this work is just starting.

Acknowledgements

The author wishes to thank J.-C. Salomon, of the Laboratoire Hydrodynamique et Sédimentologie of IFREMER, and his staff, who received him in their laboratory and allowed him to use their model. He also wishes to acknowledge support from SHOM, and particularly B. Simon who provided data on tides and programs for tidal analysis.

REFERENCES

Andrews D.G., M.E. McIntyre (1978). An exact theory of non-linear waves on Lagrangian mean flow. *J. Fluid Mech.* **89**, 4, 609-646.

Bessero M. (1979). Analyse des observations de courants première partie: analyse spectrale et analyse harmonique. Rapport no. 493 EPSHOM/OC, Brest.

Chardy P., C. Chevillon, J. Clavier (1988). Major benthic communities of the south-west lagoon of New Caledonia. *Coral Reefs* **7**, 69-75.

Debenay J.P. (1987). Sedimentology in the southern lagoon of New Caledonia, SW Pacific. *J. Coast. Res.* **3**, 1, 77-91.

Douillet P., G. Bargibant, P. Hamel, C. Hoffschir, J.L. Menou, J.L. Panché, P. Tirard (1990). Mesures de courant, de marée et de vent dans le lagon sud-ouest de Nouvelle-Calédonie. 2e partie: juillet 1989 à octobre 1990. Nouméa : ORSTOM. *Rapp. sci. tech., Sci. Mer, Biol. mar.* **58**, 722 p.

Douillet P., G. Bargibant, C. Hoffchir, C. Laboute, J.L. Menou, J.Y. Panché, P. Tirard (1989). Mesures de courant, de marée et de vent dans le lagon sud-ouest de Nouvelle Calédonie. 1ère partie: octobre 1988 à juillet 1989. Nouméa: ORSTOM. *Rapp. sci. tech., Sci. Mer, Biol. mar.* **53**, 271 p.

Foreman M.G.G., A.M. Baptista, R.A. Walters (1992). Tidal model studies of particle trajectories around a shallow coastal bank. *Atmosphere-Ocean* **30**, 1, 43-69.

Garreau P. (1993). Hydrodynamics of the North Brittany coast: a synoptic study. *Oceanologica Acta* **16**, 5-6, 469-477.

Gonella J. (1972). A rotary-component method for analysing meteorological and oceanographic vector times series. *Deep-Sea Res.* **19**, 833-846.

Jarrige F., R. Radok, G. Krause, P. Rual (1975). Courants dans le lagon de Nouméa (Nouvelle Calédonie). Déc.74-janv. 75. Rapp. ORSTOM (Nouméa) et H. Lamb. Inst. of Oceanogr., Flinders Univ. S. Australia., 6 p.

Lazure P., J.C. Salomon (1991). Coupled 2-D and 3-D modelling of coastal hydrodynamics. *Oceanologica Acta* **14**, 2, 173-180.

Longuet-Higgins M.S. (1969). On transport of mass by time-varying ocean currents. *Deep-sea Res.* **16**, 431-447.

Morlière A. (1985). Assainissement de Nouméa. Mesures de courant. *Rap. sci. tech. ORSTOM*, 50 p.

Morlière A., J.L. Crémoux (1981). Observations de courant dans le lagon, de février à août 1981. *Rap. sci. tech., ORSTOM*, 50 p.

Rougerie F. (1986). *Le lagon sud-ouest de la Nouvelle-Calédonie: spécificité hydrologique et productivité.* Paris: ORSTOM. *Études et Thèses*, 231 p.

Salomon J.-C., P. Guéguéniat, A. Orbi, Y. Baron (1988). A lagrangian model for long term tidally induced transport and mixing. Verification by artificial radionuclide concentration. *In: Radionuclides: a tool for oceanography*, J.-C Guary, P. Guéguéniat, R.S. Pentreath, eds. Elsevier Applied Science, 384-395.

Schwiderski E.W. (1981). Global Ocean tides: a detailed hydrodynamical interpolation model. *Tech. Rap.*, Nav. Surface Weapons Cent., Rahlgren, Va., 2-10.

Simon B. (1974). Calcul des constantes harmoniques de la marée. Rapport no. 122 EPSHOM/OC, Brest.

Coden OCACD 9
ISSN 0399 1784

ELSEVIER

OCEANOLOGICA ACTA

European Journal of Oceanology

Volume 21 - N° 1 - January-February 1998